Euro PM2004
Sintering

Study of Particle Rearrangements during Sintering Processes by Microfocus Computer Tomography (µ-CT)

Dr. Michael Nöthe*, Dr. Karsten Pischang*, Dr. Petr Ponížil**, Prof. Bernd Kieback***, Prof. Joachim Ohser****

** Dresden University of Technology, Dresden, Germany*
*** Tomáš Baťa University, Zlín, Czech Republic*
**** Fraunhofer-Institut für Fertigungstechnik und Angewandte Materialforschung, Dresden, Germany*
***** Darmstadt University of Applied Sciences, Darmstadt, Germany*

Abstract
Sintering processes are usually described by theories based on the observation of the well known two particle models. Such theories can give a good description of the formation of bonds, the growth of sinter necks and particle centre approach during the sintering process. Further particle motions are not considered in these models. Thus the inconsistence of the calculated and the observed shrinkage of real specimens is attributed to particle rearrangements due to the complex particle constitution. These assumed particle rearrangements inside of 3D samples are neither quantified nor proved up to now.
Microfocus computer tomography (µ-CT) is the first method to measure the positions of all individual particles inside of 3D metal powder samples. Thus the particle rearrangements due to the powder geometries like particle size distribution, irregular particle shape and inhomogeneous sample densities can be analysed in detail. Sequences of sintering stages of spherical copper powder (particle size 200…1000 µm) were prepared by frequently interrupting the sintering process. Mathematical models were used to determine the particle motions and constitutions by µ-CT images of each sintering stage. The statistical correlation of the formation and breaking of sinter necks, the rotation and motion of particles and the sample shrinkage are presented and used to elucidate the sintering process. The presented article shows the formation and breaking of individual sinter necks, the rotation of particles, a strong correlation of sample shrinkage and particle motion and that the vector fields of particle motions are irregular and not directed towards the centre of mass.

Introduction

On the one hand a basic requirement for the description of sintering processes is a detailed knowledge of the growth of contact zones between particles, as described by usual sintering models based on the description of material diffusion in two particle boundaries [1,2]. On the other hand any attempt to describe and optimize sintering processes neglecting the particle constitution results in a significant inconsistence between the behaviour of real powder samples and the theoretical predicted behaviour. This is attributed to motions of whole particles due to the complex geometry causing stress by inhomogeneous particle approach and the tendency to form low energy grain boundaries. Thus great effort has been made to achieve experimental data suitable to give a self-contained description of changes in particle constitution. Prior to the invention of µ-CT these efforts were limited to the observation of rows of metal balls, 2D models and the observation of surfaces of 3D models [3-6]. The

application of µ-CT to analyze metal powder specimens in various stages of sintering gives the first opportunity to gain quantitative experimental data about the particle motions inside of the samples, as described in the present paper.
The particle motion within the time required to perform the measurement of a µ-CT image exceeds the resolution of the image. Thus the sintering of the copper powder in a hydrogen atmosphere had to be interrupted frequently to perform the measurements at room temperature. The obtained sequences of µ-CT images were analyzed with regard to the relationship between the speed of particle motion, the change of angle between the particles (speed of rotation) and the sintering necks.

Experiments
Alumina crucibles (∅ 7 mm, 4 mm high) were filled with spherical copper particles of 200...315 µm (samples 4 and 6) or 1000 µm diameter. A diluted alcoholic solution of polyvinylpyrrolidone was used to fix the particles in their positions. The samples were analyzed in the initial stage (usually not sintered) and after the preparation of each sintering stage. The decomposition of the polyvinylpyrrolidone was performed by heating the samples (rate: 5 K/min) in a hydrogen atmosphere up to 250 °C. Finally the sintering stage was prepared by heating the sample to the respective sintering temperature (T_s) for the predetermined duration (t_s) as listed in Table 1.

Sample ID	Stage of sintering ID	T_s [°C]	t_s [h]	Remarks
1	1.0	-	-	Initial stage
	1.1	850	1	
	1.2	950	1	
	1.3	1000	1	
	1.4	1050	1	The measurement was repeated 6 times to estimate the error of the analysis
2	2.0	-	-	Initial stage
	2.1	950	1	
	2.2	1050	1	
3,4	3.0 / 4.0	-	-	Initial stage
	3.1 / 4.1	600	1	
	3.2 / 4.2	650	1	
	3.3 / 4.3	700	1	
	3.4 / 4.4	750	1	
	3.5 / 4.5	800	1	
	3.6 / 4.6	830	1	
	3.7 / 4.7	850	1	
	3.8 / 4.8	900	1	
	3.9 /4.9	950	1	
5,6	5.1 / 6.1	1050	1	Initial stage (Ar + H_2 atmosphere)
	5.2 / 6.2	1050	4	
	5.3 / 6.3	1050	4	
	5.4 / 6.4	1050	4	
	5.5	1050	1	(heating rate 2,5 K/min)

Table 1 List of samples[1]

[1] Between several measurements particles were lost. The results of measurements performed after the loss of a particle were excluded from most parts of the data analysis.

Figure 1 shows the scheme of our µ-CT system. The selected acceleration voltage of the microfocus X-ray tube (1) was set to 175 KV in order to optimize the emitted X-ray spectrum with respect to the transmission of the samples. For further improvement of the X-ray spectrum the samples 3 and 4 were measured with a 0.8 mm copper filter between the

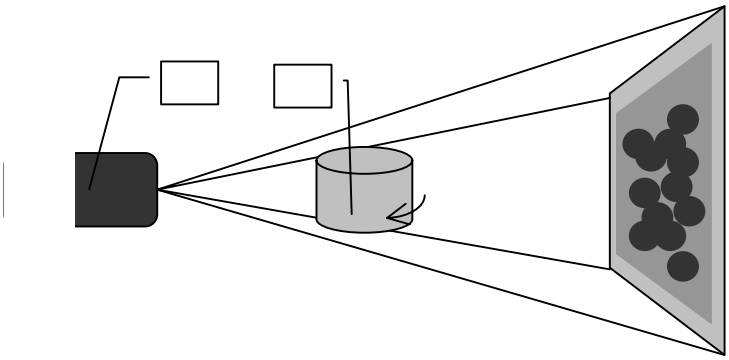

microfocus X-ray tube and the specimen. A detailed description of the beam hardening correction software is given in [7,8]. The effect of the beam hardening correction is shown in Figure 2.

Figure 1. Scheme of the µ-CT system

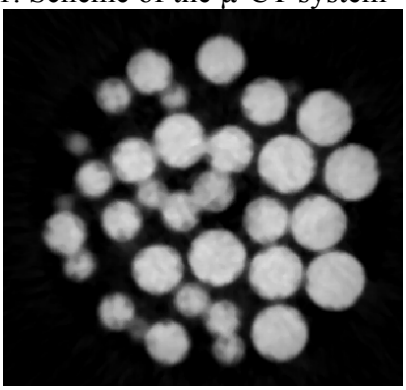

a) with edge hardening correction

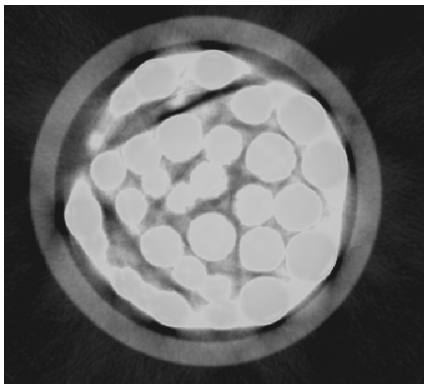

b) without edge hardening correction

Figure 2. Slices of a 3-D image

The particle centres were determined by approximating an Euclidian distance map and the determined positions were refined by the calculation of the centre of mass of a Voronoï tessellation [9]. Particles with a common tessellation boundary are neighbours. We will address connected neighbours as coordination partners or first order neighbours. Other neighbours will be referred as second order neighbours. The results of the image analysis were used to characterize the sample by the

- distance between the particles and the next neighbours,
- motion of the particles (average distance between a particle centre and the position of the centre of the same particle in the previous sintering step),
- change of the angle of particle triplets in subsequent sintering steps,
- size of the sample (length of the sample along the crucible axis),
- average coordination of the particles and
- number of new and broken connections.

Correlations between the parameters were determined for process characterization.

Results

Figure 3 shows a 3D visualization of a sintered sample. The visualisation of the particle motions inside of a sintering specimen can give a impression of the processes occurring during sintering. The observed particle motions neither straight and nor directed towards the centre of mass, indicating that sintering theories based on two particle models do not apply to the observed processes.

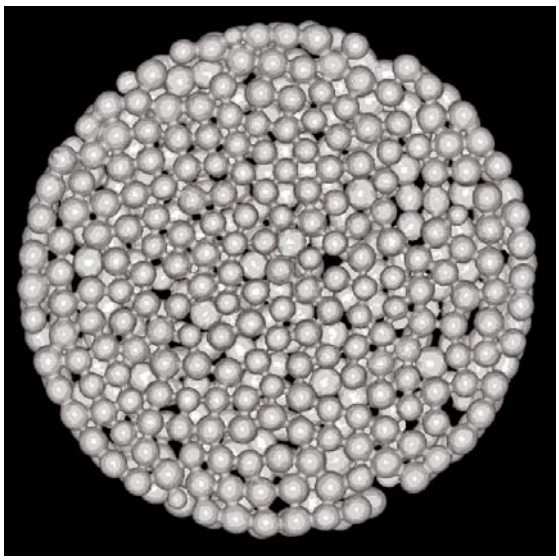

Figure 3. 3D visualization of a sintered sample

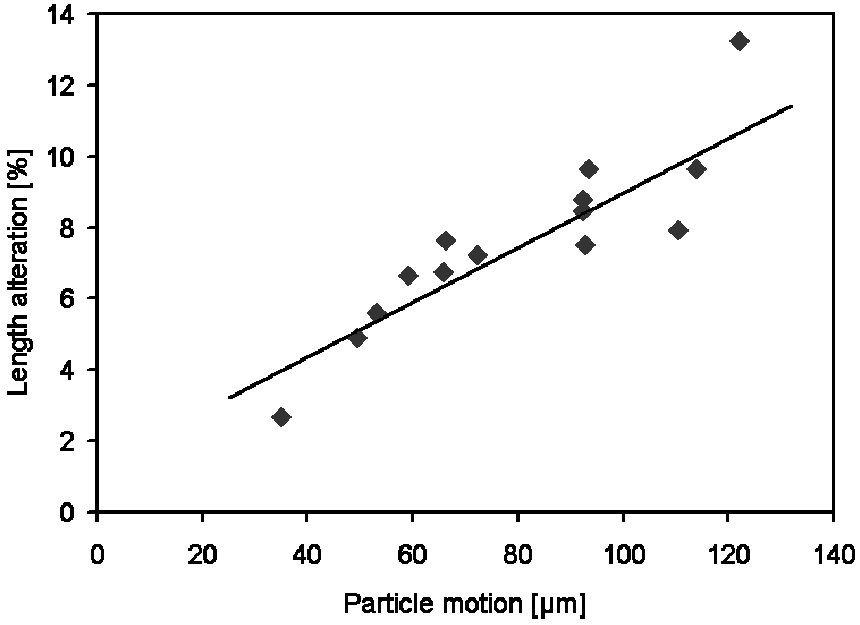

Figure 4. Relationship of sample expansion and particle motion for samples 1, 2, 3 and 5.

Furthermore, the vectors of particle motions indicate that the samples consisting of 1 mm copper balls a sample expansion and large particle motions occur during the first sintering step. To verify this relationship the sample expansions and particle motions of all sintering steps were plotted in one graph (Fig. 4). Obviously, the measured values are arranged near the inserted regression line. The analysis reveals a highly significant relationship of sample expansion and particle motion and sample expansion (less than 0.05 % probability to observe the arrangement near the regression line if the values were independent).
Figure 5 a shows the extraordinary close relationship between the change of angle in particle triplets (here used as measure of particle rotation) and the observed particle motion. Thus a causal linkage between particle motion and particle rotation must be concluded. According to literature sample expansions are attributed to the rotation of particles due to the tendency to form low energy grain boundaries. The close correlation of the sample expansion and the change of angle shown in Fig. 5 b is the first experimental verification in a 3D sample.
The analysis was extended to the forming and breaking of particle connections. The average coordination remained almost unchanged in all sintering stages. The data analysis revealed a significant correlation between the particle rotation and the disappearance of individual

contacts, Fig. 6 a. Furthermore, a correlation between new contacts and particle rotation was found, Fig. 6 b, but the probability for an accidental arrangement close to the regression line is slightly higher than 5%, i.e. is not significant. Obviously, a balanced formation and break-up of particle connections occurs during the particle rotation.

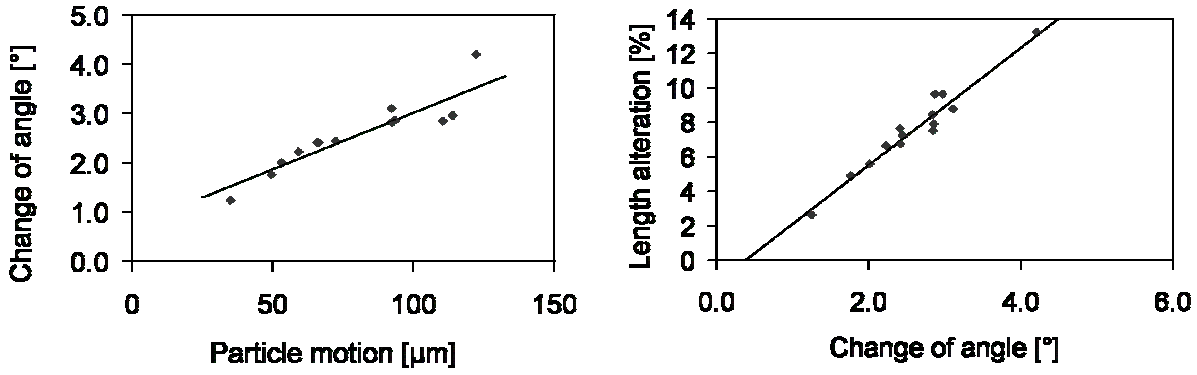

a) b)

Figure 5. Relationship of change of angle (particle rotation) and particle motion (a) and sample expansion (b) for samples 1, 2, 3 and 5

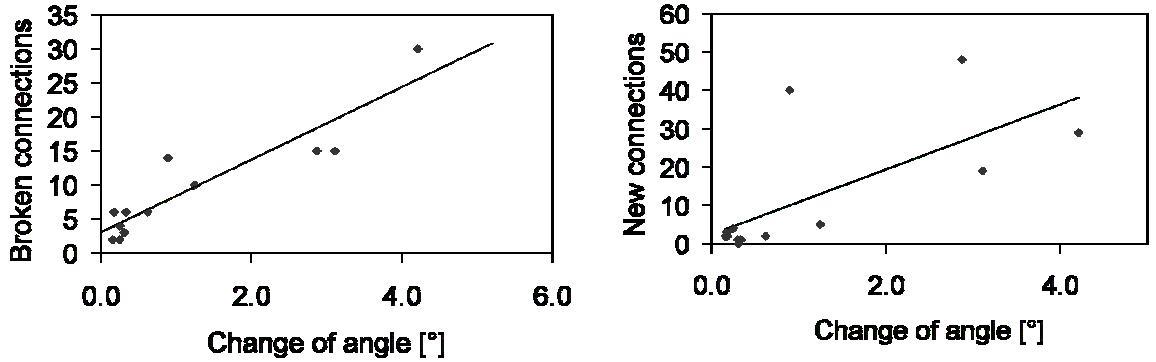

a) b)

Figure 6. Relationship of change of angle (particle rotation) and the break-up (a) and formation of particle connections (b) for samples 1, 2, 3 and 5

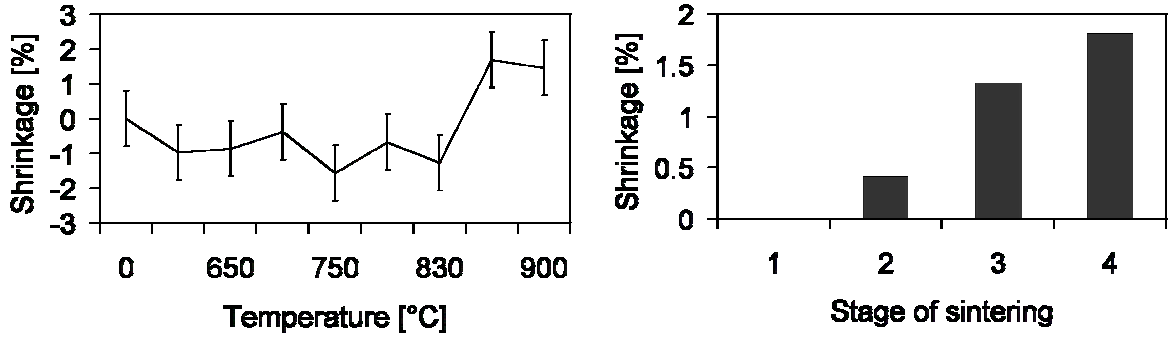

a) b)

Figure 7. Shrinkage of the samples 4 and 6

Beside the samples used for verification of tomography as suitable analysis method and for the development of data analysis first samples (4,6) consisting of 200...315 µm spherical copper particles were analyzed. Currently the data analysis is limited to the determination of the particle positions (without the possibility to track particles across consecutive sintering steps). The shrinkage of both samples is shown in Fig. 7. During the initial stages of the sintering of sample 4 (Fig. 7a) a slight expansion was observed. At 850 °C the shrinkage was 1.7%. At 900 °C no further progress of the shrinkage was observed. Sample 6 (Fig. 7b) was

sintered 1 hour before the initial measurement of a tomogram and was sintered 4 hours at 1050 °C between each measurement. This sample shows a continuous shrinkage of up to 1.8%. The analysis of the mean distance to the next neighbour shows no changes beyond the error of measurement in all sintering stages. Nevertheless the mean distance to the next neighbours behaves qualitatively similar to the shrinkage. Similar results are obtained from the power spectra of the 3D images measured on the base of fast discrete Fourier transform [9,10].

Conclusion

Due to the large particle sizes a particle centre approach was not possible. Nevertheless particle rearrangements were measured inside of 3D samples for the first time. The largest particle motions occur during the first sintering step. The close correlation between the particle motions, rotations and the sample expansion lead to the conclusion, that the particles rotate due to the desire to form low energy grain boundaries. The resulting motion causes an expansion of the specimens. A steep decrease of particle rotation occurs after the first sintering step and leads to the conclusion that an optimal particle arrangement is reached during early sintering stages.

Acknowledgements

The authors would like to thank Dr. Goebbels, Federal Institute for Materials Research and Testing for useful discussions. Furthermore, we are grateful to the Deutsche Forschungsgemeinschaft (DFG) for financial support.

References

[1] Geguzin, J.E.: Physik des Sinterns, VEB Deutscher Verlag für Grundstoffindustrie, Leipzig, 1973
[2] Schatt, W.: Sintervorgänge, VDI-Verlag 1992
[3] Wieters, K.P.: Korngrenzeneinfluß beim defektaktivierten Sintern; Habil.; TU Dresden 1989
[4] Exner, R.E.: Grundlagen von Sintervorgängen, Gebr. Borntraeger Berlin Stuttgart, 1978
[5] Kingery, W.D., Berg, M.: J. Appl. Phys. 26 (1955) 1205
[6] Schatt, W., Hinz, P.: Powder Met. Int. 20 (1988) 6, p.17
[7] Imaging systems for medical diagnostics, ed. Erich Krestel, Berlin, Munich: Siemens-Aktiengesellschaft (Abt. Verl.) 1990, ISBN 3-8009-1564-2
[8] Nöthe, M., Pischang, K., Ponížil, P., Bernhardt, R., Kieback, B.: Advances in Powder Metallurgy & Particulate Materials - 2002, ISBN: 1-878954-90-3, Part 13, pp.176-184
[9] Ohser, J. und F. Mücklich : Statistical Analysis of Materials Structures. J.Wiley & Sons, Chichester, London, New York 2000. (ISBN 0-471-97486-2)
[10] Koch, K., Ohser, J., Schladitz, K.: Adv. in Appl. Probab. 35 (2003), no. 3, pp.603-613